Cell
P R E S S

Open
ACCESS

The Ku Heterodimer and the Metabolism of Single-Ended DNA Double-Strand Breaks

Alessia Balestrini,[1] Dejan Ristic,[2] Isabelle Dionne,[3] Xiao Z. Liu,[1] Claire Wyman,[2] Raymund J. Wellinger,[3] and John H.J. Petrini[1,*]
[1]Molecular Biology Program, Sloan-Kettering Institute, New York, NY 10065, USA
[2]Department of Radiation Oncology, Erasmus Medical Center, P.O. Box 2040, 3000 CA Rotterdam, the Netherlands
[3]Département de Microbiologie et Infectiologie, Université de Sherbrooke, Sherbrooke, QC J1H 5N4, Canada
*Correspondence: petrinij@mskcc.org
http://dx.doi.org/10.1016/j.celrep.2013.05.026

SUMMARY

Single-ended double-strand breaks (DSBs) are a common form of spontaneous DNA break, generated when the replisome encounters a discontinuity in the DNA template. Given their prevalence, understanding the mechanisms governing the fate(s) of single-ended DSBs is important. We describe the influence of the Ku heterodimer and Mre11 nuclease activity on processing of single-ended DSBs. Separation-of-function alleles of *yku70* were derived that pheno-copy Ku deficiency with respect to single-ended DSBs but remain proficient for NHEJ. The Ku mutants fail to regulate Exo1 activity, and bypass the requirement for Mre11 nuclease activity in the repair of camptothecin-induced single-ended DSBs. Ku mutants exhibited reduced affinity for DNA ends, manifest as both reduced end engagement and enhanced probability of diffusing inward on linear DNA. This study reveals an interplay between Ku and Mre11 in the metabolism of single-ended DSBs that is distinct from repair pathway choice at double-ended DSBs.

INTRODUCTION

DNA double-strand breaks (DSBs) can be caused by exposure to ionizing radiation or genotoxic chemicals. DSBs spontaneously arise most commonly during DNA replication when DNA replication forks encounter a discontinuity in the template, a circumstance that leads to the formation of single-ended DSBs (Ryan et al., 1991; Shao et al., 1999; Strumberg et al., 2000). In contrast, double-ended DSBs are most likely to arise from HO endonuclease cleavage during mating-type switching, or by Spo11 at the onset of meiotic recombination (Pâques and Haber, 1999). Nonhomologous end joining (NHEJ) and homologous recombination (HR) are the two modes by which DSBs are repaired. NHEJ consists of the religation of DNA ends, with little or no DNA homology required. In *Saccharomyces cerevisiae*, the core components of NHEJ are the yKu heterodimer (yKu70-yKu80), Dnl4-Lif1, Lif2, and the Mre11 complex (which consists of Mre11, Rad50, and Xrs2) (Boulton and Jackson, 1996, 1998;
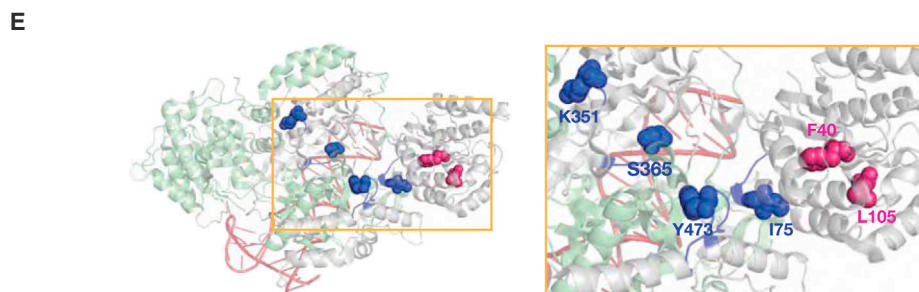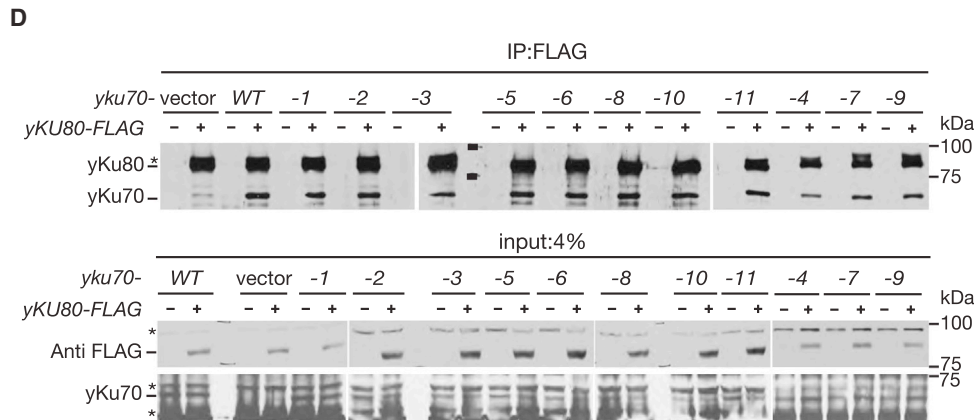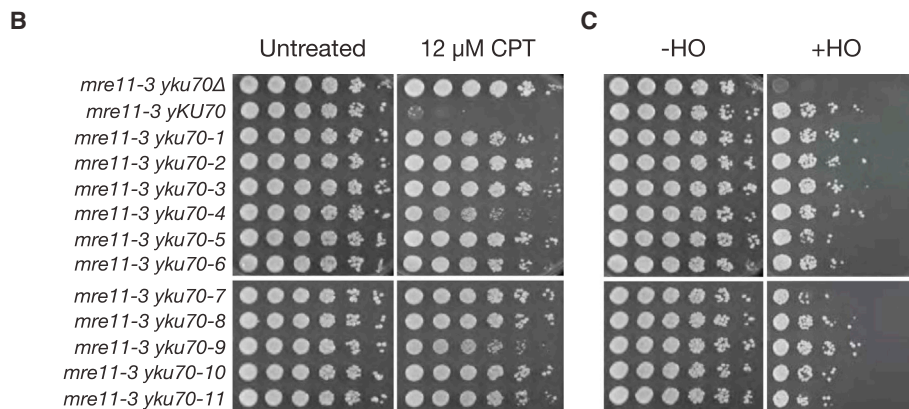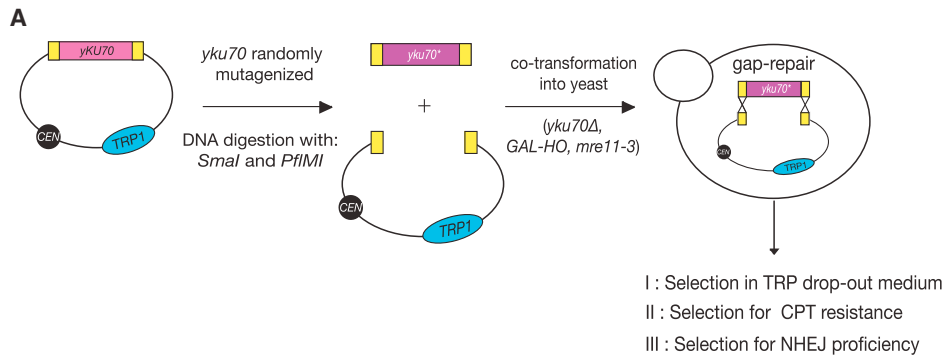
Daley et al., 2005; Frank-Vaillant and Marcand, 2001; Moore and Haber, 1996; Schär et al., 1997; Teo and Jackson, 1997).

HR is initiated by resection of the 5′ strand of the DSB end to generate a 3′ single-stranded DNA (ssDNA) tail that subsequently invades homologous duplex DNA (usually a sister chromatid) and copies information from that template to restore the site of the break (Heyer et al., 2010). Recent in vivo data suggest a two-step mechanism for DSB resection. In the first step, a short (∼50 base) 3′ ssDNA overhang is generated by the Mre11 complex and Sae2. In the second step, long-range resection is effected by two pathways, one dependent on Exo1 and the other dependent on Sgs1 and Dna2 (Gravel et al., 2008; Mimitou and Symington, 2008; Zhu et al., 2008).

The choice between NHEJ and HR depends on the phase of the cell cycle. 5′-to-3′ resection of DSB ends is inhibited in G1, when cyclin-dependent kinase (CDK) activity is low, and is favored in G2/M phase, when CDK activity is high (Aylon et al., 2004; Barlow et al., 2008; Ira et al., 2004). Consequently, HR occurs primarily in S and G2 phases of the cell cycle when a sister chromatid is available as a repair template, whereas NHEJ is generally restricted to G1 phase.

With regard to single-ended DSBs, the issue of pathway choice is less relevant because these breaks are unlikely to be substrates for NHEJ, and are primarily repaired by invasion of the intact sister chromatid to initiate leading and lagging strand DNA synthesis from the point of invasion (Lydeard et al., 2007, 2010). The possible fate(s) of the end thus extended includes copying to the end of the chromosome and dissociation and reinvasion of the same or alternative templates downstream of the initial break site (Llorente et al., 2008; Smith et al., 2007). In mammalian cells, it also appears that the extended DSB end may dissociate and be resolved by NHEJ (Richardson and Jasin, 2000), although such events have not been noted in *S. cerevisiae*.

The Ku heterodimer is an abundant nuclear protein that binds with high affinity to duplex DNA ends, hairpin loops, and single-strand nicks in a sequence-independent manner (Blier et al., 1993; Foster et al., 2011; Griffith et al., 1992; Mimori and Hardin, 1986). Structural analysis of the human Ku heterodimer revealed a ring-like conformation formed by the interaction of Ku70 and Ku80 subunits, which provides the structural basis for Ku to bind to DNA ends, as well as the ability of Ku to slide along duplex DNA (de Vries et al., 1989; Walker et al., 2001; Yaneva et al., 1997).

CrossMark

A

yku70 randomly mutagenized

DNA digestion with:
SmaI and PflMI

co-transformation into yeast
(yku70Δ, GAL-HO, mre11-3)

gap-repair

I : Selection in TRP drop-out medium
II : Selection for CPT resistance
III : Selection for NHEJ proficiency

B

Untreated   12 μM CPT

mre11-3 yku70Δ
mre11-3 yKU70
mre11-3 yku70-1
mre11-3 yku70-2
mre11-3 yku70-3
mre11-3 yku70-4
mre11-3 yku70-5
mre11-3 yku70-6

mre11-3 yku70-7
mre11-3 yku70-8
mre11-3 yku70-9
mre11-3 yku70-10
mre11-3 yku70-11

C

-HO   +HO

D

IP:FLAG

input:4%

E

K351   F40
S365
Y473   I75   L105

(legend on next page)

Several lines of evidence suggest that Ku and the Mre11 complex antagonize each other at DNA ends to influence the choice between NHEJ and HR; however, the significance of this interplay relative to the cell-cycle phase as the primary determinant of pathway choice is not clear (Clerici et al., 2008; Wu et al., 2008; Zhang et al., 2001). Also unclear is the relevance of Mre11 nuclease activity and Sae2 protein in pathway choice. Previous studies that examined this relationship predominantly used *mre11Δ* mutants, in which Ku binding to DNA ends prevents long-range resection at an HO-induced double-ended DSB. Mre11 nuclease activity and Sae2 appear to be dispensable for resection of enzymatically induced double-ended DSBs, whereas nuclease activity may be required for chemically complex "dirty" ends, such as those produced by ionizing radiation (Mimitou and Symington, 2010; Shim et al., 2010).

The Ku heterodimer is also required for telomere maintenance (Wellinger and Zakian, 2012). The telomeric functions of Ku are genetically separable from its role in NHEJ (Bertuch and Lundblad, 2003; Driller et al., 2000; Roy et al., 2004; Stellwagen et al., 2003; Taddei et al., 2004). These findings suggest a "two-face" model in which the Ku70 surface is oriented toward the DNA terminus and influences NHEJ, whereas the Ku80 surface is oriented inward and promotes interactions with telomeric heterochromatin (Ribes-Zamora et al., 2007).

Having previously demonstrated that yKu deficiency suppressed the IR sensitivity of *mre11Δ* mutants in *S. cerevisiae* (Bressan et al., 1999), we recently found that yKu70 deficiency suppressed the sensitivity of a nuclease-dead *mre11* mutant (*mre11-3*) to CPT (Foster et al., 2011). The CPT sensitivity of *mre11-3* was unaffected by Dnl4 deficiency, indicating that the genetic interaction observed between *yku70Δ* and *mre11-3* is independent of NHEJ. Exo1 activity was required for suppression in *mre11-3 yku70Δ* mutants, suggesting that Ku inhibition of Exo1 contributes to *mre11-3* sensitivity. Moreover, because CPT-induced damage requires DNA replication (Pommier et al., 2006), this genetic interaction reveals an S-phase-specific, NHEJ-independent role of the Ku heterodimer (Foster et al., 2011).

In this study, we performed a genetic screen to isolate *yKU70* alleles that phenocopied *yku70Δ* with respect to the suppression of *mre11-3* CPT sensitivity while leaving NHEJ functions intact. The *yKU70* gene products exhibited reduced affinity for DNA ends and an increased probability to slide inward once bound. Accordingly, the ability of mutant gene products to inhibit Exo1 activity in vitro was reduced. These results suggest a model in

which the Mre11 complex and Ku regulate the metabolism of single-ended DSBs in S phase, a process with the potential to influence DNA repair outcomes as well as checkpoint activities.

RESULTS

Screen for *yku70* Separation-of-Function Mutations

The goal of this study was to examine the NHEJ-independent function(s) of the yeast Ku heterodimer at single-ended DSBs in S phase cells (Foster et al., 2011). The first step toward this goal was to construct alleles of *yKU70* that separated its functions in S phase from those involved in NHEJ. We mutagenized *yKU70* and screened for CPT resistance in an *mre11-3 yku70Δ* strain, followed by a secondary screen for NHEJ proficiency (Figure 1A). This strategy excludes silent mutants in the first step because they will complement the *yku70Δ* mutation and thereby cause CPT sensitivity. Null mutations will be excluded in the secondary screen because the transformants will remain NHEJ deficient. A library of *yku70* mutants (hereafter *yku70**) was created by PCR amplification of the *yKU70* open reading frame (ORF) followed by gap repair into a centromeric plasmid upon transformation of *mre11-3 yku70Δ* cells. The resulting *yku70* mre11-3* transformants were plated on solid media containing 12 μM CPT. From ~30,000 primary transformants, 2,300 CPT-resistant colonies (~7%) were obtained.

CPT-resistant transformants were subsequently screened for NHEJ proficiency. In the *yku70Δ mre11-3* strain used, the *HML* and *HMR* elements are deleted so that the DSB created by HO must be repaired by NHEJ in order for the cells to retain viability (Lee et al., 1998). This two-step screening led to the identification of 89 mutants that conferred CPT resistance and NHEJ proficiency to *mre11-3 yku70Δ* cells. *yku70** alleles with more than one amino acid change were excluded from further analysis, and 11 *yKU70* mutations, six of which also appeared among the multiply mutated alleles (*yku70-1* to *yku70-11*; Tables 1 and S1) were retained for further analysis (Figures 1B and 1C). yKu70 and yKu80 coimmunoprecipitated in all of the 11 retained mutants (Figure 1D). Conversely, mutations that drastically affected the expression level of *yku70** gene products were deficient in NHEJ (Figures S1A and S1B). Finally, as expected from previous analyses (Foster et al., 2011), *yku70** mutants also conferred CPT resistance upon *yku70Δ sae2Δ* cells (Figures S1C and S1D).

The *S. cerevisiae* Ku heterodimer is moderately conserved relative to its human counterpart, for which the crystal structure

Figure 1. *yku70* Mutants Are Deficient for Ku-Specific S Phase Function but Proficient for NHEJ

(A) Schematic illustration of the genetic screen used to identify *yKU70* separation-of-function mutants. The screen was performed using JPY5025, a *yku70Δ mre11-3* yeast strain carrying *GAL-HO hmlΔ hmrΔ* in a W303+ background.

(B) Centromeric plasmids carrying *yku70** alleles were transformed in JPY5025 strain (see Extended Experimental Procedures). Exponentially growing cells of the indicated genotypes were 1:5 serially diluted and spotted on DO-TRP lactate in the presence or absence of CPT (12 μM).

(C) The same yeast strains were plated onto solid media containing either glucose or galactose to repress (−HO) or induce (+HO) expression of HO endonuclease.

(D) Integrity of the yKu70-yKu80 complex in yeast strain JPY5097 transformed with empty vector (vector) or vector expressing yKu70 wild-type (WT) or yKu70* mutants (*yku70−*). FLAG-tagged (+) or untagged (−) yKu80 was immunoprecipitated with anti-FLAG antibody and yKu70, yKu80 proteins were analyzed by western blot (WB) with anti-yKu70-yKu80 antibody. Input yKu80-FLAG and yKu70 were analyzed by WB (* indicates nonspecific band).

(E) Position of human Ku70 residues that correspond to the residues mutated in *yku70** alleles mapped on the Ku-DNA crystal structure (Walker et al., 2001). hKu70 and hKu80 are shown in gray and green, respectively, and the DNA is in red. The predicted positions of the yKu70 mutations are shown by colored spheres (blue spheres map inside or adjacent to the protein loops, and magenta spheres map to β sheets).

See also Figures S1 and S3 and Tables 1 and S1.

Table 1. Residues of *yku70** Alleles that Are Conserved in Human, Related to Figure 1

yku70* Mutants[a]	Mutated Amino Acids in yKu70[b]	Corresponding Sites in hKu70[c]	Domain[d]
yku70-2	R369C	K351	β-barrel
yku70-3	**L100S**	**L105**	α/β
yku70-5	**Y494N**	**Y473**	C-terminal
yku70-6	**F34S**	**F40**	α/β
yku70-10	**S384R**	**S365**	β-barrel
yku70-11	V70D	I75	α/β

[a]The *yku70** alleles carrying a single point mutation, in residues conserved from yeast to human, are ordered by crescent number.
[b,c]Identical amino acids are in bold and similar amino acids are in regular font. Similar amino acids were grouped as follows: [isoleucine (I), leucine (L), valine (V)]; [aspartic acid (D), glutamic acid (E), asparagine (N), glutamine (Q)]; [alanine (A), glycine (G)]; [serine (S), threonine (T)]; [phenylalanine (F), tyrosine (Y), tryptophan (W)]; [cysteine (C), methionine (M)]; [arginine (R), lysine (K), histidine (H)]; [proline (P)].
[d]Domains in yeast and human Ku70 that each mutated amino acid is part of.

has been obtained (Walker et al., 2001). Among the 11 *yku70** mutants that were retained, six fell within residues that were conserved in the human Ku70 protein (Table 1) and were subjected to further characterization. The mutations did not cluster to a particular domain (Figure 1E), although two mutations (Figure 1E, magenta spheres) localized to β sheets A and B that lie within the N-terminal α/β domains of yKu70.

*yku70** Mutants Are Defective in Telomere End Protection

We have suggested that *yku70** mutations affect the activity of the Ku heterodimer at single-ended DSBs that arise when the replisome encounters discontinuity in the template (see Figure 6). In this context, we reasoned that telomeres might analogize single-ended DSBs, and that *yku70** alleles may also affect telomere maintenance. The telomere length of *yku70** mutants was measured by southern blotting of DNA extracted from freshly dissected spores. In all six conserved mutants, telomere length was reduced (Figure 2A), indicating that the activity of *yku70** mutants at telomeric ends, as well as single-ended DSBs in S phase, was affected. Telomere shortening in *yku70** was dependent on Exo1, as telomere length was partially restored in *yku70** *exo1Δ* double mutants (Figure 2A). In addition, quantitation of telomeric ssDNA overhangs revealed a 3- to 7-fold increase in ssDNA signal in *yku70** (Figures 2B and 2C). Thus, telomere overhang length and to a lesser extent telomere length in *yku70** mutants exhibited a similar dependence on Exo1 compared with their ability to suppress *mre11-3* CPT sensitivity (Figure S2A).

Previous studies have identified separation-of-function *yku70* and *yku80* alleles in which NHEJ functions are intact but telomere protection is compromised (Bertuch and Lundblad, 2003; Lopez et al., 2011; Ribes-Zamora et al., 2007). Given that the *yku70** alleles also separate NHEJ and telomeric functions, we tested two of the previously identified alleles for their ability to suppress *mre11-3* CPT sensitivity. In each case, these mutants phenocop-

ied *yku70** mutants (Figures 2D and S2C). Conversely, mutations affecting yKu80 interaction interface with telomeric heterochromatin or the yKu70 interface required for NHEJ did not suppress *mre11-3* CPT sensitivity (Figure S2B). These data suggest that Ku's functions at single-ended DSBs are similar to its role in protecting telomeric DNA ends, and that in both contexts, its functions are separable from NHEJ.

Biochemical Analysis of *yku70** Gene Products

To understand the mechanistic basis of the *yku70** phenotype, we analyzed the behavior of the mutant gene products in vitro. *yku70-5* and *yku70-10* were coexpressed in bacteria with *yKU80* and purified to near homogeneity (Figure 3A). The yKu70-5 and yKu70-10 proteins contain mutations in the loops adjacent to the C-terminal and β-barrel domains, respectively (Figure 1E; Walker et al., 2001; Zhang et al., 2001).

The DNA-binding behavior of the *yku70** gene products was assessed in two contexts: filter binding assays and electrophoretic mobility shift assays (EMSAs; for in vitro assays, yKu70, yKu70-5, and yKu70-10 refer to a heterodimer of yKu70-yKu80, yKu70-5-yKu80, and yKu70-10-yKu80, respectively). For the filter binding assay, increasing concentrations of the yKu complex were incubated with a dsDNA fragment of 25 bp representing a single Ku-binding site (de Vries et al., 1989; Kysela et al., 2003; Ma and Lieber, 2001) as well as a 465 bp fragment to which multiple Ku proteins could bind (Figures 3B and 3C). The DNA-binding affinity of yKu70-5 and yKu70-10 for the single-site substrate was reduced (for the short substrate, $K_D = 1.4$ nM and $K_D = 0.8$ nM, respectively) relative to the wild-type protein ($K_D = 0.2$ nM). The apparent K_D on the longer DNA substrate was reduced to 1.6 nM (yKu70-5) and 0.5 nM (yKu70-10) nM, whereas it remained unaltered in the wild-type protein ($K_D = 0.2$ nM; Figure 3C).

Although it exhibits a strong preference for blunt DNA ends, the Ku heterodimer is capable of sliding inward from the end to bind internal sites (Blier et al., 1993). EMSAs were carried out to determine whether the stoichiometry of DNA binding was altered in yKu70-5 or yKu70-10. Increasing concentrations of yKu were added to a radiolabeled dsDNA substrate, and complex formation was analyzed by EMSA (Figures 3D and 3E). The radiolabeled substrate was an 80 bp blunt DNA molecule that is capable of binding three Ku molecules (Blier et al., 1993; Ma and Lieber, 2001). Accordingly, with wild-type protein we observed three shifted bands, likely representing DNA bound to one, two, or three Ku molecules. At a ratio of two yKu complexes per substrate molecule, (Figure 3D, lane 3), the predominant product was the doubly bound species, whereas the singly bound substrate was ~8-fold less abundant. At a 5-fold ratio of yKu to DNA, the singly bound species was absent, and the triply and doubly bound forms were 40% and 35% of the total substrate (Figure 3D, lane 5). In contrast, triply bound yKu70-10 or yKu70-5 complexes were not detected at any concentration. The relative fraction of doubly bound forms was greatest at 5-fold excess, but was reduced by 11% and 30% relative to wild-type (compare lane 5, 9, and 13). Hence, the suppression of *mre11-3* CPT sensitivity by *yku70** mutants is correlated with reduced DNA binding of the yKu heterodimer. Given that suppression requires Exo1, this observation further suggests
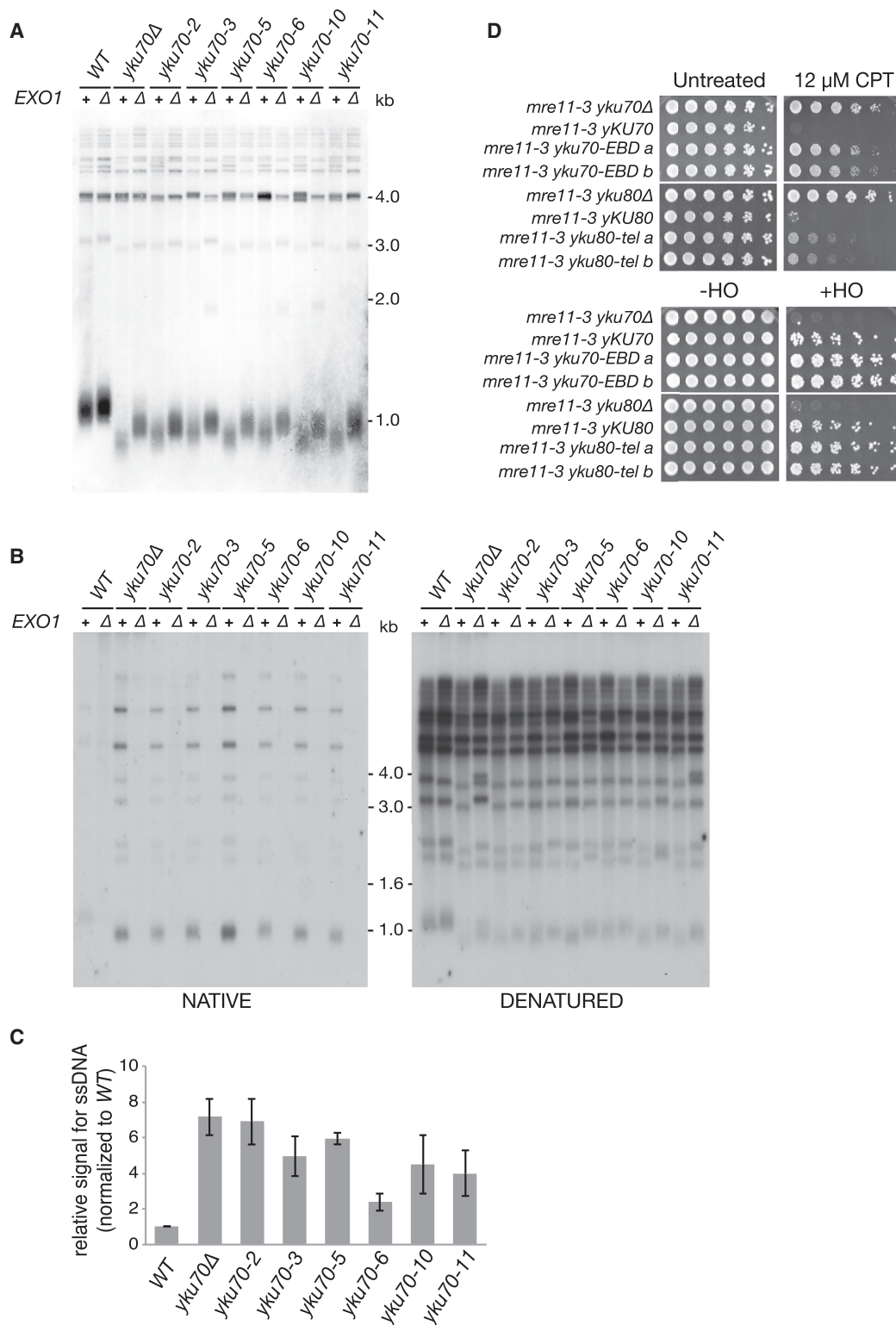
Figure 2. Rescue of *mre11-3* CPT Sensitivity and Telomere Shortening in *yku70** Alleles Require EXO1

(A) Telomere length analysis of the indicated *yku70** mutants. Plasmids bearing *yku70** alleles or control vectors were transformed into *yku70Δ* or *yku70Δ exo1Δ* strains. After 60 generations, telomeric sequences were detected by southern blot analysis of *XhoI*-digested genomic DNA.

(B) Telomeric G-overhang assay. Genomic DNA isolated from *yku70Δ* or *yku70Δ exo1Δ* strains transformed with CEN plasmids containing the indicated *yku70** alleles were digested with *XhoI* restriction enzyme and separated on a 0.7% agarose gel. The gel on the left was treated as a nondenaturing gel and hybridized to

(legend continued on next page)

that reduced affinity of yKu interferes with its inhibition of Exo1 activity.

Given the decrement in DNA binding exhibited by the *yku70** gene products, a quantitative analysis of NHEJ proficiency was undertaken. A direct view of the DSB repair kinetics of an HO-induced DSB was obtained by quantitative PCR (qPCR) following transient expression of HO (Hohl et al., 2011). Cells expressing the integrated *yku70** alleles *yku70-5* and *yku70-10* were placed in galactose-containing media for 15 min. HO expression was then suppressed by the addition of glucose. qPCR with primers spanning the DSB site 4 and 6 hr after HO suppression was carried out to quantify DSB rejoining (Figure 3F). At 6 hr in glucose, 14% of wild-type cells, 8% of *yku70-10* cells, and 9% of *yku70-5* cells had repaired HO DSB, whereas DSBs persisted in *yku70Δ* cells and apparently were degraded, as qPCR signals decreased over the course of the experiment (−6%). These data demonstrate that *yku70-5* and *yku70-10* are proficient in NHEJ, and indicate that the process of NHEJ is not strongly affected by the reduced affinity of the Ku heterodimer for DNA ends. Further supporting this interpretation, we found that the NHEJ junctions in *yku70-5* and *yku70-10* were indistinguishable from those of wild-type cells following chronic exposure to galactose (Figure S3A), whereas the predominant outcome in *yku70Δ* colonies was extensive deletions (>500 bp) or inactivation of HO expression (data not shown).

We have proposed that these mutants reveal an NHEJ-independent function of Ku that is specific to single-end DSBs and is the predominant role for Ku in S phase cells. This hypothesis predicts that whereas the *yku70** mutants phenocopy *yku70Δ* in S phase, they will not do so in G1 cells. In Ku-deficient cells, induction of the HO endonuclease leads to Exo1-dependent DSB resection and activation of Rad53 within 1 hr of DSB formation (Clerici et al., 2008). Wild-type, *yku70Δ*, *yku70-5*, and *yku70-10* strains were arrested in G1 and the HO endonuclease was induced. Rad53 phosphorylation was monitored for up to 4 hr after HO induction (Figures S3B and S3C). As expected, Rad53 phosphorylation appeared 60 min after HO induction in the *yku70Δ* strain, but was detectable at low levels in similarly treated wild-type cells beginning at 2 hr postinduction (Figure S3C). In both *yku70-10* and *yku70-5* strains, modest Rad53 activation occurred by 2 hr postinduction, as in the wild-type strain. Hence, the phenotype of *yku70-5* and *yku70-10* alleles is similar to wild-type in G1 cells, but phenocopies *yku70Δ* with respect to its effect on *mre11-3* in S phase.

yKu70* Mutants and Exo1 Activity In Vitro

The requirement for Exo1 in the suppression of *mre11-3* CPT sensitivity is likely attributable to Ku-mediated inhibition of Exo1 at DSB ends. To test that interpretation, we employed a blunt-ended dsDNA 80-mer, biotinylated at the 5′ end of one strand (Figure S4A). The complementary strand is radiolabeled 50 bases in from the end, so a 5′-to-3′ resection of that strand will produce labeled intermediates from 79 to 30 bases long, culminating in the release of the labeled mononucleotide (Figure 4A). Streptavidin binding blocks resection of the biotinylated strand, restricting access of Exo1 to the internally labeled strand. Thus prepared, the labeled 80-mer was incubated with yKu for 60 min prior to the addition of Exo1, and the reaction was inactivated at certain time points after Exo1 addition. Reaction products were resolved on a denaturing gel, and the appearance of labeled AMP was monitored. In the presence of wild-type yKu heterodimer, 6% of the substrate was degraded to produce AMP within 30 s, rising slightly to 9% upon further incubation to 60 min. However, in the absence of yKu, 36% of the substrate was converted by 30 s, increasing to 72% at 15 min and to 77% at 60 min when the curve reached a plateau (Figures 4B, 4C, S4B, and S4C). These data demonstrate that yKu inhibits Exo1-dependent resection in this setting, as was previously shown with the corresponding human proteins (Sun et al., 2012).

The extent of Exo1 inhibition by complexes containing yKu70-5 and yKu70-10 mutants correlated roughly with the severity of their DNA-binding defect, with yKu70-10 inhibited to a greater extent than yKu70-5. Nevertheless, AMP release was 3- to 4-fold higher than observed in the wild-type at 30 s, and approximated the levels observed in the control reaction lacking yKu altogether by 15 min (Figures 4B and 4C). As expected, the detected increase in AMP correlated quantitatively with the decrease in signal of the initial DNA substrate (Figure S4D). Similar trends in inhibition of lambda exonuclease were observed with wild-type and mutant yKu complexes, indicating that yKu-mediated inhibition of resection is not species specific (Figure S4E).

SFM Analysis of DNA Binding by Mutant Ku Complexes

Taken together with previously described genetic interactions among Ku, Exo1, and *mre11-3* (Foster et al., 2011), the failure of *yku70** gene products to inhibit Exo1 as described above supports a model in which Ku binds single-ended DSBs and regulates the action of Exo1 in a manner antagonized by Mre11 nuclease activity. To gain further insight into the DNA-binding properties underlying the behavior of the mutant proteins, we carried out scanning force microscopy (SFM) to examine the binding of yKu heterodimers to a 1.8 kb DNA substrate (Figures 5A, 5B, and S5). DNA was incubated for 30 min with 8-fold molar excess of yKu (1 nM versus 8 nM) prior to deposition and analysis.

Approximately 800 DNA molecules were examined in each experiment (Table S2); 85% of the substrate was bound by

the end-labeled CA-oligo. The amount of telomeric ssDNA was quantitated before the gel was denatured and probed with the same telomere probe to reveal the total amount of telomeric DNA (right).

(C) Ratio of telomeric ssDNA to total telomeric DNA, normalized to WT. Error bars indicate SDs of three independent quantifications.

(D) CPT sensitivity of *mre11-3 yku70* DNA end-binding-defective mutants and *yku80* telomere mutants. Top: serial dilutions of JPY5025 strain containing the indicated *yku70* or *yku80* alleles on a CEN plasmid were spotted onto DO-TRP lactate in the presence or absence of CPT. Bottom: NHEJ assays as described in Figure 1C. *yku70* and *yku80* alleles nomenclature: *yku70-EBD* (DNA end-binding deficient: *yku70-R456E* spores a and b; Lopez et al., 2011); *yku80-tel* (*yku80-P437L* spores a and b; Bertuch and Lundblad, 2003).
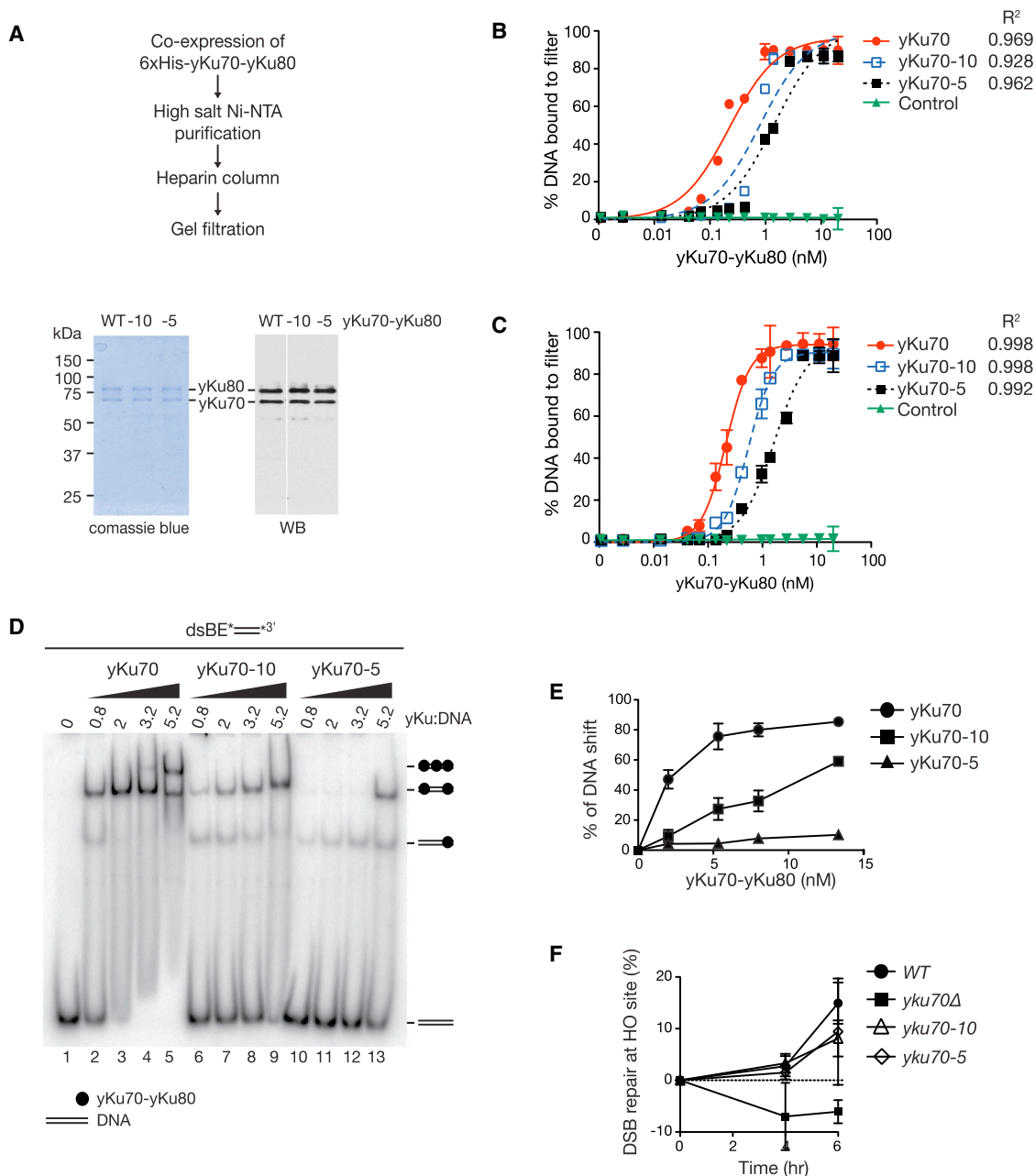
See also Figure S2.

Figure 3. Mutations in yKu70 Loops Reduce the Affinity of the yKu Heterodimer for DNA Ends

(A) yKu70 wild-type and −5 and −10 mutants were purified to homogeneity in complex with yKu80. The purified complexes were resolved by SDS-PAGE gel, analyzed by WB, and stained with Coomassie blue.

(B and C) Analysis of DNA-yKu interaction by filter binding assay. Increasing amounts of the indicated recombinant yKu complexes were incubated overnight with 0.1 nM of 25 bp (B) and 465 bp (C) 5′-labeled dsDNA. Radiolabeled DNA bound to protein was retained on nitrocellulose filter and quantified by scintillation counter. Denatured boiled yKu70 was used as control. Error bars represent the SD of three independent experiments and are smaller than the symbols when not evident. R^2 is the coefficient of determination.

(D) Gel mobility shift assay of yKu binding to 80 bp dsDNA blunt ends (dsBE). The DNA concentration was 2.5 nM in all binding reactions, whereas Ku concentrations are represented by the Ku to DNA molar ratios. Bands representing free DNA or one, two, and three yKu molecules in complex with DNA are indicated.

(E) Quantification of the gel in (D). Error bars represent the SD of three independent experiments and are smaller than the symbols when not evident.

(F) NHEJ repair kinetics after acute (15 min) HO induction were determined by qPCR in *yKU70* (JPY5726), *yku70-5* (JPY5730), and *yku70-10* (JPY5728) integrated in the endogenous *yKU70* locus in a *GAL-HO hmlΔ hmrΔ* strain W303+ background. *yku70Δ* (JPY5735) was used as negative control. Cells were cultivated for another 4 or 6 hr in glucose medium after HO induction, and repair was monitored with primer flanking the HO site.
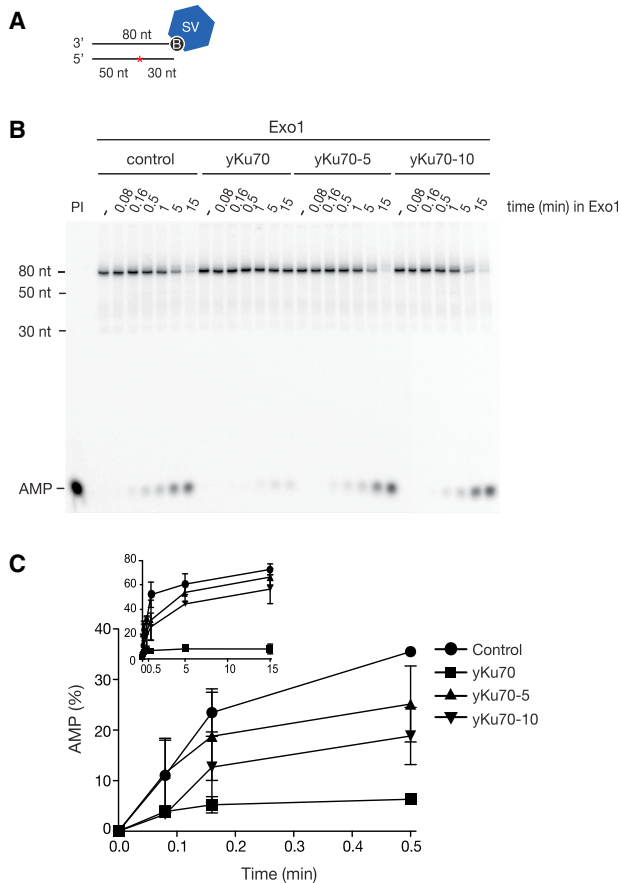
See also Figure S3.

Figure 4. yKu70* Mutants Fail to Block Exo1-Dependent Resection In Vitro

(A) Representation of the DNA substrate used in the resection assay in (B). 5′ biotinylated 80-mer oligonucleotide was annealed to an equally long internally labeled oligonucleotide that would release free AMP upon Exo1 resection (* indicates the position of ^{32}P on DNA). B, biotin; SV, streptavidin.

(B) Biotinylated DNA substrate (1 nM) was preincubated with streptavidin, followed by the presence or absence (control) of the indicated yKu complexes (5 nM). The kinetics of resection by Exo1 (3 nM) was determined at the times indicated by separation of DNA on denaturing gel, and the resection products were visualized with the PhosphorImager system. An 80 bp oligo 5′ labeled on the first adenine was digested with Phosphodiesterase I (PI) and the AMP generated was used as the control for Exo1 resection.

(C) The percentage of generated AMP from the experiment shown in (B) is plotted as a function of time. A magnification of the graph in the first 0.5 min is represented to show the curve slope, and the full graph is reported in small scale. Error bars represent the SD from three independent experiments and are smaller than the symbols when not evident.

See also Figure S4.

wild-type yKu, 94% of which was at DNA ends. The majority of wild-type yKu-DNA complexes had yKu and both ends of the substrate (Figures 5A and 5B). These DNA-binding properties are similar to those of human Ku70-Ku80 (Mimori and Hardin, 1986; Paillard and Strauss, 1991; Yaneva et al., 1997). In contrast, yKu70-5- and yKu70-10-containing heterodimeric complexes exhibited a propensity for sliding inward once they were bound to the substrate. Whereas the mutant complexes were each bound to one or both ends 57% of the time, 39%

and 23% of protein-bound DNA molecules also contained internally bound Ku complexes of yKu70-5 and yKu70-10, respectively (Figures 5B and S5). The fraction of substrate molecules that were devoid of yKu complexes was the same for wild-type and yKu70-10 (14%), whereas 68% of the substrate molecules were devoid of yKu70-5-containing complexes (Table S2). These data indicate that reduced affinity in yKu70-5 and yKu70-10 is also associated with diffusion inward from the DNA end. This raises the possibility that failure to inhibit Exo1 in vivo is attributable to Ku sliding inward on single-end DSBs in addition to a reduced probability of end binding.

DISCUSSION

We previously established evidence for an NHEJ-independent role of the Ku heterodimer at single-ended DSBs (Foster et al., 2011). This interpretation was based on the observation that the CPT sensitivity of nuclease-deficient *mre11-3* mutants is suppressed by Ku, but not by DNA ligase IV deficiency. That suppression was dependent on Exo1, suggesting a role for Ku in modulating the processing of single-ended DSBs. In this study, we provide mechanistic insight into the function of the Ku heterodimer in that setting. We identified *yku70* separation-of-function mutants (*yku70** mutants) that have intact NHEJ but phenocopy *yku70Δ* with respect to suppression of *mre11-3* CPT sensitivity. Biochemical analysis revealed that the yKu heterodimer inhibited Exo1-mediated degradation of DSB ends, and that inhibition by *yku70** gene products was reduced. The effect on Exo1 inhibition was correlated with reduced affinity of the yKu heterodimer for DSB ends. The reduced affinity was manifest as both a reduction in end binding of, and a propensity of the mutant heterodimer to diffuse inward on linear DNA. These data suggest a model wherein the interplay between Mre11 and yKu at single-ended DSBs influences the activity of Exo1 during DNA replication (Figure 6).

In vegetatively growing cells, spontaneous DSBs most frequently arise during DNA replication when the replisome encounters a discontinuity in the template. In this scenario, the resulting lesion is a single-ended DSB (Figure 6), indicating that the mechanisms by which cells mitigate this lesion are likely relevant to maintaining the genome integrity of replicating cells.

The mechanisms of single-ended DSB repair differ fundamentally from those of double-ended DSB. First, single-ended DSBs cannot be readily repaired by NHEJ due to the lack of a second DNA end to which the single-ended DSB can be joined (Cromie et al., 2001). Second, in the course of HR-based repair of double-ended DSBs, capture of the second end is temporally coupled to the initial strand invasion event (Allers and Lichten, 2001; Bzymek et al., 2010; Hunter and Kleckner, 2001). Temporal coupling of this nature is not possible with a single-ended DSB. In the course of repair by break-induced replication (BIR), the extended DSB end can reinvade the acceptor chromatid (Llorente et al., 2008; Smith et al., 2007), but such an event would by definition be uncoupled from the initial invasion. A "second end" could also be created by the arrival of the replisome from an adjacent origin of replication, again uncoupled from the initial invasion event. Recent data suggest that DSB formation may induce the activation of local dormant origins (Doksani et al.,
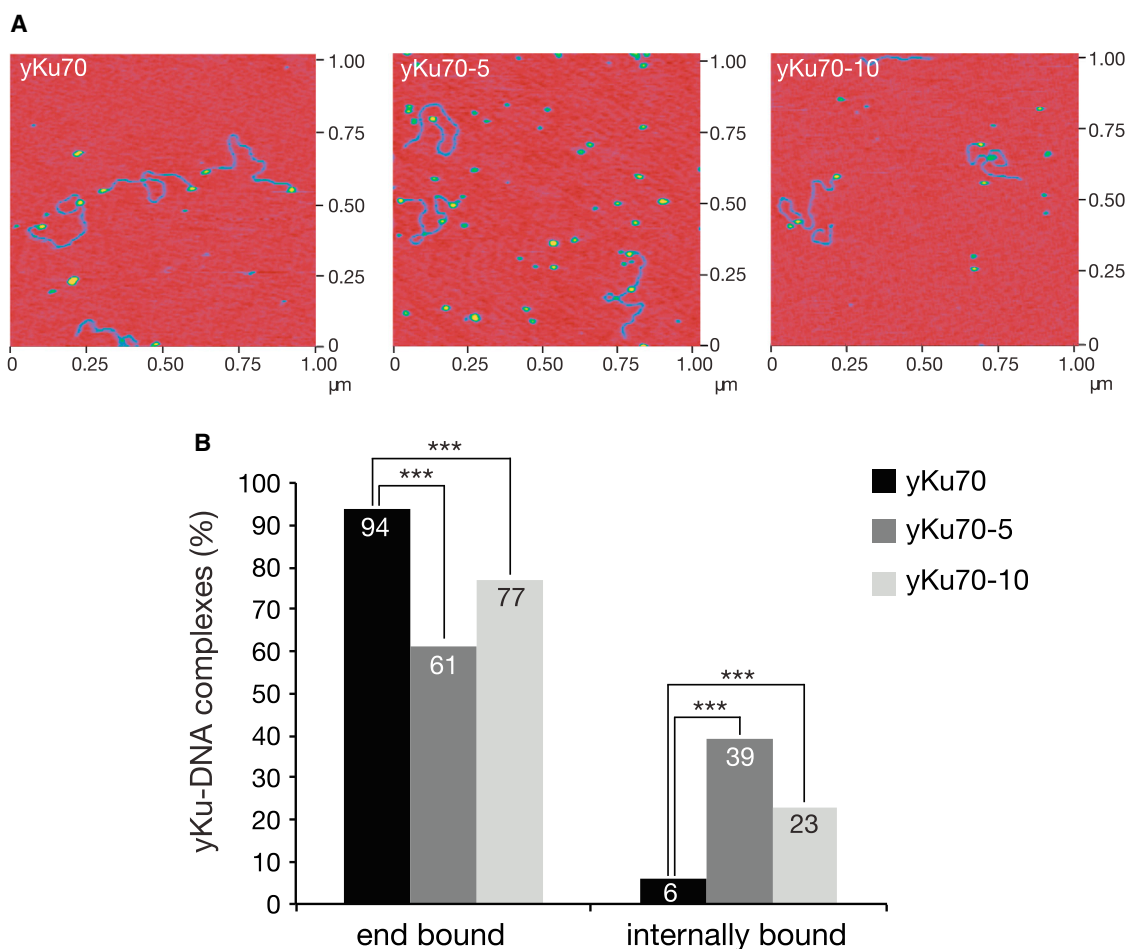
A

B

Figure 5. Interaction of yKu70-yKu80 Heterodimers with Linear Duplex DNA Molecules

Nucleoprotein complexes formed between blunt-ended linear DNA (1,821 bp) and the indicated yKu70-yKu80 heterodimers were visualized by SFM as described in Experimental Procedures.

(A) Representative SFM images. Left panel: DNA-yKu70; central panel: DNA-yKu70-5; right panel: DNA-yKu70-10. The percentages of the total yKu complexes bound to DNA at either internal sites or DNA ends are reported in Table S2.

(B) Graph representing the percentages of the total yKu complexes bound to DNA at either internal sites or DNA ends. Fisher's exact test was performed on the number of yKu molecules bound to DNA, at DNA ends and internal sites, between yKu70 and yKu70-5, and yKu70 and yKu70-10. In all cases, the p value for a two-sided test is <0.0001 (***). Percentages of the total yKu complexes bound to DNA at either internal sites or DNA ends are shown in the graph. See also Figure S5.

2009), perhaps enhancing the effectiveness of this mechanism. Nevertheless, it is unlikely that this scenario could lead to temporal coupling of the two single-ended DSBs formed. Hence, even though the molecular bases of the antagonism between Ku and the Mre11 complex at double- and single-ended DSBs may share some similarities, the potential repair mechanisms and outcomes are distinct.

In this study, we present evidence that the interplay between the Ku heterodimer and Mre11 at single-ended DSBs influences the action of Exo1 at the break, thereby affecting its repair. Ku and Mre11 appear to govern the choice between HR and NHEJ at double-ended DSBs, such as those induced by the HO endonuclease (Shim et al., 2010), but the significance of their interplay at single-ended DSBs is likely confined to regulating the extent of resection. Previous analyses support the idea that end

resection influences BIR. Whereas extensive resection has an inhibitory effect, mutations in *EXO1* and *SGS1*, which strongly impair resection, increase the frequency of BIR events (Marrero and Symington, 2010). These observations resonate well with the phenotype of *mre11-3*, as well as its genetic interaction with *yku70Δ*. In *mre11-3*, resection is impaired, and CPT treatment induces mitotic recombination at doses that have no effect on wild-type cells. Deletion of *yKU70* in *mre11-3* reduces the induction to essentially wild-type levels. The data presented here support the interpretation that the induction of mitotic recombination is reduced in *mre11-3 yku70Δ* double mutants because resection is restored in that setting. Conversely, CPT does not induce mitotic recombination in *yku70Δ*, suggesting that the increase in resection resulting from yKu deficiency suppresses BIR (Foster et al., 2011).
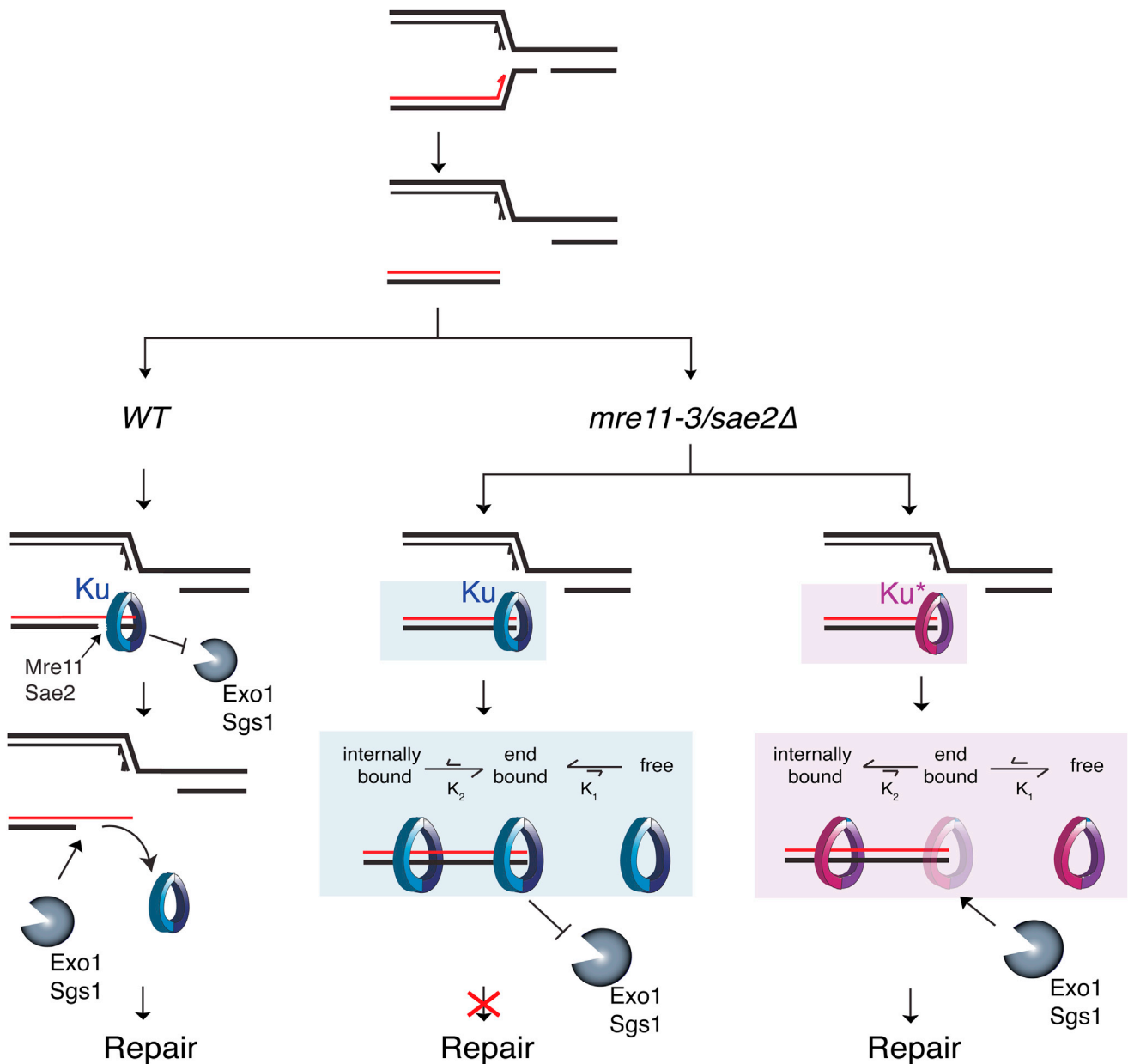
Figure 6. Model Depicting the Effect of Mre11/Sae2 and the yKu Complex in Coordinating Exo1-Dependent Processing and Repair of Single-Ended DSBs

We propose that in the presence of replication-induced single-ended DSBs, Mre11 and Sae2 repress Ku binding at DNA ends, thereby promoting Exo1 recruitment and resection. To explain the molecular basis of yKu70 suppression of single-ended DSB resection, we postulate two nonexclusive scenarios responsible for a reduction of Ku affinity to DNA ends. In our model, a stable binding of the wild-type yKu heterodimer (dark-and light-blue oval structure) to single-ended DSB ends occurs as consequence of an equilibrium maintained between two Ku-DNA binding modes (K_1 and K_2). On this basis, reduced yKu affinity for DNA ends may take place as a consequence of mutations that increase the yKu off-rate and/or the ability of Ku to diffuse inward on the DNA molecule (Ku*: pink and purple oval structure). The reduction in Ku-DNA end-binding stability can be explained by a structural analysis of the Ku mutants. The use of a software (Rosetta Common) to predict the effect(s) of single-point mutations on a protein structure highlighted a shift in the overall backbone conformation (data not shown) of the Ku heterodimer caused by mutation in Ku70. A consequent reduction in the persistency of Ku at DNA ends translates to a failure to protect DNA ends from Exo1 exonuclease activity. We cannot test Sgs1's role in this model because of the synthetic interaction with *mre11-3* (Foster et al., 2011). K_1 and K_2 represent the equilibrium constant of Ku-DNA binding modes.

We propose a model for Ku's action at single-ended DSBs (Figure 6). At the single-ended DSB, the probability of Ku engagement is reduced by the initial Mre11- or Sae2-mediated incision event, which produces a 50- to 100-base overhang (Ku binding to an ssDNA overhang is significantly less avid than that to a blunt end; Foster et al., 2011). Exo1 next carries

out bulk resection of the DNA end to promote BIR (Figure 6). In cells expressing *mre11-3* and *sae2Δ*, the first incision step is impaired and Ku binding is not inhibited, which in turn limits Exo1 resection, resulting in sensitivity to CPT. As with the induction of mitotic recombination by CPT, *mre11-3* CPT sensitivity is abolished by yKu70 deletion (Foster et al., 2011).

Collectively, the data obtained here indicate that the mechanistic basis for the suppression of *mre11-3* CPT sensitivity in *yku70* mre11-3* double mutants is the reduction in the end-binding affinity of yKu70*-containing complexes. As in *yku70Δ*, the lower affinity of these complexes effectively bypasses the requirement for the Mre11 incision step and permits Exo1 to resect DNA. In addition, the data clearly support the interpretation that Ku's effect on Exo1 at single-ended DSBs is analogous to its effect at telomeric DNA ends (Vodenicharov et al., 2010).

In addition to the reduced probability of end engagement, the propensity of yKu70*-containing heterodimers to slide inward from the DSB end may also account for the failure to inhibit Exo1-mediated resection. This possibility suggests that some fraction of yKu may be threaded onto DNA during chromosome DNA replication. It is conceivable that trapped complexes could pose a physical impediment to replication forks or the transcriptional machinery. Previous data obtained in human cells and *Xenopus laevis* egg extracts showed that Ku80 becomes polyubiquitinated when bound to a DSB, promoting its removal from DNA (Feng and Chen, 2012; Postow et al., 2008). Whether a similar mechanism is operative in *S. cerevisiae* has not been established.

The data presented here clearly show that the Mre11 complex, the Ku heterodimer, and Exo1 act interdependently to coordinate the repair of single-ended DSBs. Because it ultimately regulates the formation of ssDNA, this interplay has the potential to also modulate checkpoint activation. Hence, this NHEJ-independent function of Ku is likely to exert a diverse impact on the metabolism of single-ended DSBs and the response to DNA replication-associated DSBs. Given that the Ku complex is present in organisms such as *S. cerevisiae* in which NHEJ is relatively insignificant for survival, we suggest that the selection for this function of the Ku heterodimer described here may account for its broad phylogenetic conservation.

EXPERIMENTAL PROCEDURES

The *yku70** alleles are listed in Table S1. The yeast strains, plasmids, and antibodies used in this work are listed in Table S3, Table S4, and the Extended Experimental Procedures, respectively. Protein purification, immunoprecipitation of protein complexes, and biochemical and genetic assays were conducted as described in the Extended Experimental Procedures.

Identification of *yku70** Alleles
JPY5025 strain was cotransformed with PCR randomly mutagenized *yKU70* fragments and pRS314 vector digested with *SmaI* and *PflMI*. JPY5025 strain transformed with digested vector was used as a negative control. Transformants were replica plated on media containing 12 μM CPT. The *yku70** mutants were screened for their ability to rescue the CPT sensitivity of *mre11-3* cells. Positive clones that confer resistance of *mre11-3* to CPT contain both vectors that carry mutated *yKU70* and empty vectors that behave as *yku70* null. A total of 2,300 candidates resistant to CPT were individually streaked on DO-TRP lactate plates containing galactose or glucose for expression or repression, respectively, of HO endonuclease. Clones growing on galactose were recov-

ered after 4 days of incubation at 30°C. Positive clones were retested on galactose media after loss of *TRP1* plasmid by 5-fluoroanthranilic acid (FAA). This would eliminate positive clones that confer both resistance of *mre11-3* to CPT and NHEJ proficiency due to selection of suppressor mutations in the genome. Clones that reacquired sensitivity to HO expression in the absence of *TRP1* centromeric-*yku70** vectors were isolated and the plasmids recovered. Plasmid purification from yeast cells was performed with the use of a Miniprep kit (QIAGEN). Yeast O/N culture (3 ml) was resuspended in 250 μl of P1 buffer in the presence of 250 μl of glass beads (425–600 μm). Cells were mechanically lysed by vortexing at max rpm for 5 min at room temperature, and subsequent purification was performed according to the manufacturer's instructions. Vectors were eluted from spin columns with 50 μl H₂O, and 2 μl of the eluted vectors were transformed in chemically competent DH5α bacterial strain. Amplified vectors purified by the Miniprep kit were sequenced for mutations in *yKU70*. A total of 89 *yku70* mutants were isolated. Combinations of single- and multiple-point mutations were identified. Among 11 single-point mutation alleles (*yku70-1* to *yku70-11*), six whose mutated residues were conserved in mouse and human (*yku70-2*, *yku70-3*, *yku70-5*, *yku70-6*, *yku70-10*, and *yku70-11*) were further characterized.

REFERENCES

Allers, T., and Lichten, M. (2001). Differential timing and control of noncrossover and crossover recombination during meiosis. Cell *106*, 47–57.

Aylon, Y., Liefshitz, B., and Kupiec, M. (2004). The CDK regulates repair of double-strand breaks by homologous recombination during the cell cycle. EMBO J. *23*, 4868–4875.

Barlow, J.H., Lisby, M., and Rothstein, R. (2008). Differential regulation of the cellular response to DNA double-strand breaks in G1. Mol. Cell *30*, 73–85.

Bertuch, A.A., and Lundblad, V. (2003). The Ku heterodimer performs separable activities at double-strand breaks and chromosome termini. Mol. Cell. Biol. *23*, 8202–8215.

Blier, P.R., Griffith, A.J., Craft, J., and Hardin, J.A. (1993). Binding of Ku protein to DNA. Measurement of affinity for ends and demonstration of binding to nicks. J. Biol. Chem. *268*, 7594–7601.

Boulton, S.J., and Jackson, S.P. (1996). Saccharomyces cerevisiae Ku70 potentiates illegitimate DNA double-strand break repair and serves as a barrier to error-prone DNA repair pathways. EMBO J. *15*, 5093–5103.

Boulton, S.J., and Jackson, S.P. (1998). Components of the Ku-dependent non-homologous end-joining pathway are involved in telomeric length maintenance and telomeric silencing. EMBO J. *17*, 1819–1828.

Bressan, D.A., Baxter, B.K., and Petrini, J.H. (1999). The Mre11-Rad50-Xrs2 protein complex facilitates homologous recombination-based double-strand break repair in Saccharomyces cerevisiae. Mol. Cell. Biol. *19*, 7681–7687.

Bzymek, M., Thayer, N.H., Oh, S.D., Kleckner, N., and Hunter, N. (2010). Double Holliday junctions are intermediates of DNA break repair. Nature *464*, 937–941.

Clerici, M., Mantiero, D., Guerini, I., Lucchini, G., and Longhese, M.P. (2008). The Yku70-Yku80 complex contributes to regulate double-strand break processing and checkpoint activation during the cell cycle. EMBO Rep. *9*, 810–818.

Cromie, G.A., Connelly, J.C., and Leach, D.R. (2001). Recombination at double-strand breaks and DNA ends: conserved mechanisms from phage to humans. Mol. Cell *8*, 1163–1174.

Daley, J.M., Palmbos, P.L., Wu, D., and Wilson, T.E. (2005). Nonhomologous end joining in yeast. Annu. Rev. Genet. *39*, 431–451.

de Vries, E., van Driel, W., Bergsma, W.G., Arnberg, A.C., and van der Vliet, P.C. (1989). HeLa nuclear protein recognizing DNA termini and translocating on DNA forming a regular DNA-multimeric protein complex. J. Mol. Biol. *208*, 65–78.

Doksani, Y., Bermejo, R., Fiorani, S., Haber, J.E., and Foiani, M. (2009). Replicon dynamics, dormant origin firing, and terminal fork integrity after double-strand break formation. Cell *137*, 247–258.

Driller, L., Wellinger, R.J., Larrivee, M., Kremmer, E., Jaklin, S., and Feldmann, H.M. (2000). A short C-terminal domain of Yku70p is essential for telomere maintenance. J. Biol. Chem. *275*, 24921–24927.

Feng, L., and Chen, J. (2012). The E3 ligase RNF8 regulates KU80 removal and NHEJ repair. Nat. Struct. Mol. Biol. *19*, 201–206.

Foster, S.S., Balestrini, A., and Petrini, J.H. (2011). Functional interplay of the Mre11 nuclease and Ku in the response to replication-associated DNA damage. Mol. Cell. Biol. *31*, 4379–4389.

Frank-Vaillant, M., and Marcand, S. (2001). NHEJ regulation by mating type is exercised through a novel protein, Lif2p, essential to the ligase IV pathway. Genes Dev. *15*, 3005–3012.

Gravel, S., Chapman, J.R., Magill, C., and Jackson, S.P. (2008). DNA helicases Sgs1 and BLM promote DNA double-strand break resection. Genes Dev. *22*, 2767–2772.

Griffith, A.J., Craft, J., Evans, J., Mimori, T., and Hardin, J.A. (1992). Nucleotide sequence and genomic structure analyses of the p70 subunit of the human Ku autoantigen: evidence for a family of genes encoding Ku (p70)-related polypeptides. Mol. Biol. Rep. *16*, 91–97.

Heyer, W.D., Ehmsen, K.T., and Liu, J. (2010). Regulation of homologous recombination in eukaryotes. Annu. Rev. Genet. *44*, 113–139.

Hohl, M., Kwon, Y., Galván, S.M., Xue, X., Tous, C., Aguilera, A., Sung, P., and Petrini, J.H. (2011). The Rad50 coiled-coil domain is indispensable for Mre11 complex functions. Nat. Struct. Mol. Biol. *18*, 1124–1131.

Hunter, N., and Kleckner, N. (2001). The single-end invasion: an asymmetric intermediate at the double-strand break to double-holliday junction transition of meiotic recombination. Cell *106*, 59–70.

Ira, G., Pellicioli, A., Balijja, A., Wang, X., Fiorani, S., Carotenuto, W., Liberi, G., Bressan, D., Wan, L., Hollingsworth, N.M., et al. (2004). DNA end resection, homologous recombination and DNA damage checkpoint activation require CDK1. Nature *431*, 1011–1017.

Kysela, B., Doherty, A.J., Chovanec, M., Stiff, T., Ameer-Beg, S.M., Vojnovic, B., Girard, P.M., and Jeggo, P.A. (2003). Ku stimulation of DNA ligase IV-dependent ligation requires inward movement along the DNA molecule. J. Biol. Chem. *278*, 22466–22474.

Lee, S.E., Moore, J.K., Holmes, A., Umezu, K., Kolodner, R.D., and Haber, J.E. (1998). Saccharomyces Ku70, mre11/rad50 and RPA proteins regulate adaptation to G2/M arrest after DNA damage. Cell *94*, 399–409.

Llorente, B., Smith, C.E., and Symington, L.S. (2008). Break-induced replication: what is it and what is it for? Cell Cycle *7*, 859–864.

Lopez, C.R., Ribes-Zamora, A., Indiviglio, S.M., Williams, C.L., Haricharan, S., and Bertuch, A.A. (2011). Ku must load directly onto the chromosome end in order to mediate its telomeric functions. PLoS Genet. *7*, e1002233.

Lydeard, J.R., Jain, S., Yamaguchi, M., and Haber, J.E. (2007). Break-induced replication and telomerase-independent telomere maintenance require Pol32. Nature *448*, 820–823.

Lydeard, J.R., Lipkin-Moore, Z., Sheu, Y.J., Stillman, B., Burgers, P.M., and Haber, J.E. (2010). Break-induced replication requires all essential DNA replication factors except those specific for pre-RC assembly. Genes Dev. *24*, 1133–1144.

Ma, Y., and Lieber, M.R. (2001). DNA length-dependent cooperative interactions in the binding of Ku to DNA. Biochemistry *40*, 9638–9646.

Marrero, V.A., and Symington, L.S. (2010). Extensive DNA end processing by exo1 and sgs1 inhibits break-induced replication. PLoS Genet. *6*, e1001007.

Mimitou, E.P., and Symington, L.S. (2008). Sae2, Exo1 and Sgs1 collaborate in DNA double-strand break processing. Nature *455*, 770–774.

Mimitou, E.P., and Symington, L.S. (2010). Ku prevents Exo1 and Sgs1-dependent resection of DNA ends in the absence of a functional MRX complex or Sae2. EMBO J. *29*, 3358–3369.

Mimori, T., and Hardin, J.A. (1986). Mechanism of interaction between Ku protein and DNA. J. Biol. Chem. *261*, 10375–10379.

Moore, J.K., and Haber, J.E. (1996). Cell cycle and genetic requirements of two pathways of nonhomologous end-joining repair of double-strand breaks in Saccharomyces cerevisiae. Mol. Cell. Biol. *16*, 2164–2173.

Paillard, S., and Strauss, F. (1991). Analysis of the mechanism of interaction of simian Ku protein with DNA. Nucleic Acids Res. *19*, 5619–5624.

Pâques, F., and Haber, J.E. (1999). Multiple pathways of recombination induced by double-strand breaks in Saccharomyces cerevisiae. Microbiol. Mol. Biol. Rev. *63*, 349–404.

Pommier, Y., Barcelo, J.M., Rao, V.A., Sordet, O., Jobson, A.G., Thibaut, L., Miao, Z.H., Seiler, J.A., Zhang, H., Marchand, C., et al. (2006). Repair of topoisomerase I-mediated DNA damage. Prog. Nucleic Acid Res. Mol. Biol. *81*, 179–229.

Postow, L., Ghenoiu, C., Woo, E.M., Krutchinsky, A.N., Chait, B.T., and Funabiki, H. (2008). Ku80 removal from DNA through double strand break-induced ubiquitylation. J. Cell Biol. *182*, 467–479.

Ribes-Zamora, A., Mihalek, I., Lichtarge, O., and Bertuch, A.A. (2007). Distinct faces of the Ku heterodimer mediate DNA repair and telomeric functions. Nat. Struct. Mol. Biol. *14*, 301–307.

Richardson, C., and Jasin, M. (2000). Coupled homologous and nonhomologous repair of a double-strand break preserves genomic integrity in mammalian cells. Mol. Cell. Biol. *20*, 9068–9075.

Roy, R., Meier, B., McAinsh, A.D., Feldmann, H.M., and Jackson, S.P. (2004). Separation-of-function mutants of yeast Ku80 reveal a Yku80p-Sir4p interaction involved in telomeric silencing. J. Biol. Chem. *279*, 86–94.

Ryan, A.J., Squires, S., Strutt, H.L., and Johnson, R.T. (1991). Camptothecin cytotoxicity in mammalian cells is associated with the induction of persistent double strand breaks in replicating DNA. Nucleic Acids Res. *19*, 3295–3300.

Schär, P., Herrmann, G., Daly, G., and Lindahl, T. (1997). A newly identified DNA ligase of Saccharomyces cerevisiae involved in RAD52-independent repair of DNA double-strand breaks. Genes Dev. *11*, 1912–1924.

Shao, R.G., Cao, C.X., Zhang, H., Kohn, K.W., Wold, M.S., and Pommier, Y. (1999). Replication-mediated DNA damage by camptothecin induces phosphorylation of RPA by DNA-dependent protein kinase and dissociates RPA:DNA-PK complexes. EMBO J. *18*, 1397–1406.

Shim, E.Y., Chung, W.H., Nicolette, M.L., Zhang, Y., Davis, M., Zhu, Z., Paull, T.T., Ira, G., and Lee, S.E. (2010). Saccharomyces cerevisiae

Mre11/Rad50/Xrs2 and Ku proteins regulate association of Exo1 and Dna2 with DNA breaks. EMBO J. *29*, 3370–3380.

Smith, C.E., Llorente, B., and Symington, L.S. (2007). Template switching during break-induced replication. Nature *447*, 102–105.

Stellwagen, A.E., Haimberger, Z.W., Veatch, J.R., and Gottschling, D.E. (2003). Ku interacts with telomerase RNA to promote telomere addition at native and broken chromosome ends. Genes Dev. *17*, 2384–2395.

Strumberg, D., Pilon, A.A., Smith, M., Hickey, R., Malkas, L., and Pommier, Y. (2000). Conversion of topoisomerase I cleavage complexes on the leading strand of ribosomal DNA into 5′-phosphorylated DNA double-strand breaks by replication runoff. Mol. Cell. Biol. *20*, 3977–3987.

Sun, J., Lee, K.J., Davis, A.J., and Chen, D.J. (2012). Human Ku70/80 protein blocks exonuclease 1-mediated DNA resection in the presence of human Mre11 or Mre11/Rad50 protein complex. J. Biol. Chem. *287*, 4936–4945.

Taddei, A., Hediger, F., Neumann, F.R., Bauer, C., and Gasser, S.M. (2004). Separation of silencing from perinuclear anchoring functions in yeast Ku80, Sir4 and Esc1 proteins. EMBO J. *23*, 1301–1312.

Teo, S.H., and Jackson, S.P. (1997). Identification of Saccharomyces cerevisiae DNA ligase IV: involvement in DNA double-strand break repair. EMBO J. *16*, 4788–4795.

Vodenicharov, M.D., Laterreur, N., and Wellinger, R.J. (2010). Telomere capping in non-dividing yeast cells requires Yku and Rap1. EMBO J. *29*, 3007–3019.

Walker, J.R., Corpina, R.A., and Goldberg, J. (2001). Structure of the Ku heterodimer bound to DNA and its implications for double-strand break repair. Nature *412*, 607–614.

Wellinger, R.J., and Zakian, V.A. (2012). Everything you ever wanted to know about Saccharomyces cerevisiae telomeres: beginning to end. Genetics *191*, 1073–1105.

Wu, D., Topper, L.M., and Wilson, T.E. (2008). Recruitment and dissociation of nonhomologous end joining proteins at a DNA double-strand break in Saccharomyces cerevisiae. Genetics *178*, 1237–1249.

Yaneva, M., Kowalewski, T., and Lieber, M.R. (1997). Interaction of DNA-dependent protein kinase with DNA and with Ku: biochemical and atomic-force microscopy studies. EMBO J. *16*, 5098–5112.

Zhang, Z., Zhu, L., Lin, D., Chen, F., Chen, D.J., and Chen, Y. (2001). The three-dimensional structure of the C-terminal DNA-binding domain of human Ku70. J. Biol. Chem. *276*, 38231–38236.

Zhu, Z., Chung, W.H., Shim, E.Y., Lee, S.E., and Ira, G. (2008). Sgs1 helicase and two nucleases Dna2 and Exo1 resect DNA double-strand break ends. Cell *134*, 981–994.